Desalination and Water Treatment
www.deswater.com

doi:10.5004/dwt.2018.22959

131 (2018) 43–49
November

Adsorption kinetics of polyethersulfone membrane-supported hydrogels

Aleksandar Stajčić[a,*], Dragutin Nedeljković[a], Vesna Panić[b], Ivana Radović[b], Aleksandar Grujić[a], Jasna Stajić-Trošić[a], Radmila Jančić-Heinemann[c]

[a]*Institute of Chemistry, Technology and Metallurgy, University of Belgrade, Njegoševa 12, 11000 Belgrade, Serbia, Tel./Fax +381 11 3370 412, email: astajcic@tmf.bg.ac.rs (A. Stajčić), Tel./Fax +381 11 3370 412, email: dragutin@tmf.bg.ac.rs (D. Nedeljković), Tel./Fax +381 11 3370 412, email: gruja@tmf.bg.ac.rs (A. Grujić), Tel./Fax +381 11 3370 412, email: jtrosic@tmf.bg.ac.rs (J. Stajić-Trošić)*
[b]*Innovation Center of the Faculty of Technology and Metallurgy,University of Belgrade, Karnegijeva 4, 11000 Belgrade, Serbia, Tel./Fax +381 11 3370 805, email: vpanic@tmf.bg.ac.rs (V. Panić), Tel./Fax +381 11 3370 616, email: iradovic@tmf.bg.ac.rs (I. Radović)*
[c]*Faculty of Technology and Metallurgy, University of Belgrade, Karnegijeva 4, 11000 Belgrade, Serbia, Tel./Fax +381 11 3303 602, email: radica@tmf.bg.ac.rs (R. Jančić-Heinemann)*

Received 16 March 2018; Accepted 14 August 2018

ABSTRACT

This study presents the route for preparation of the membrane-supporting materials with good mechanical behavior and adsorption properties that provide functionality and are easy to use in various environments. Polyethersulfone (PES) membrane-supported hydrogels were prepared *via* liquid phase inversion process with photopolymerization and monomer crosslinking. The obtained membranes had asymmetric structure containing dense skin on the top of a porous hydrogel as it is verified by scanning electron microscopy. Software analysis of the pore size revealed that fine pores enabled availability of the membrane active centers to metal cations. The membranes with a higher content of the polymer showed significantly improved mechanical properties compared with commonly used ion exchange membranes, which is crucial for the wastewater treatment application. Adsorption kinetics analysis showed that the hydrogel-rich bottom layer has significantly higher adsorption ability in comparison to the top layer. Adsorption kinetics of the bottom side was described by the first-order kinetics model, whereas for the the top side, phase-boundary controlled reaction model was used.

Keywords: Membrane formation; Hydrogel; AMPS; Photopolymerization; Adsorption kinetics

1. Introduction

The development of chemical technology and the diversity of industrial chemical processes in the past decades have generated the issue of waste waters which consist either or both of organic and inorganic non degradable pollutants [1]. An interdisciplinary field of membrane technology and separation processes has found its place in industrial development due to the possibility of membranes' versatile application, and nowadays this industry is expanding rapidly. As in the case of many other products, synthetic membranes have been inspired by biomimetic approach, relying on biological membranes [2].

Hydrogels represent the new class of the membrane materials [3]. The advantages of hydrogels are insolubility in water, large adsorption capacity and the possibility of functionalization [4,5]. Their ability to swell can be applied in bioseparation processes, controlled release, tissue engineering, pollution control, etc. The special issue in the pollution control processes is the removal of heavy metal ions [6,7]. Different blends of adsorptive polymers have given promising results for the elimination of heavy metal ions from water, especially in the case of Cu(II) removal [8]. On the other hand, despite the excellent adsorption properties, relatively poor mechanical properties often reduce

*Corresponding author.

the application field of these polymers. Therefore, the balance between chemical and mechanical properties is very important parameter that qualifies the hydro gel membranes for many uses.

A wide range of different polymer materials have been used for the preparation of membranes [9,10]. Among them,polysulphones are the most common, due to their high chemical and thermal stability. Diffusion induced phase separation (DIPS) is the most frequently used technique for the preparation of asymmetric membranes based on polymers [12–15]. This technique is based on the casting of polymer solution on support followed by the phase separation with the addition of a non-solvent for hydrogel. Another possible approach for the preparation of polymeric membranes is the use of photoirradiation applied on different types of precursors [16]. Irradiation can be used to initiate polymerization if the precursor is monomer or cross-linking if the precursor is polymer. The main advantage of this process is the construction of the cross-linked membranes in one step. Disadvantages of such systems lie in their poor mechanical properties in swollen state (when the adsorption properties are remarkable and tendency to crumble under real operating conditions [11]. Nevertheless, modification of hydrogels with mechanically superior polymer could significally improve their mechanical performance without disrupting adsorption ability.

This study presents the preparation and characterization of polymer membranes for ultrafiltration separation processes obtained by the combination of photoirradiation and liquid phase inversion. The main advantages of the membrane structure obtained in this manner besides easy handling are notably enhanced mechanical properties. The obtained membranes have substantially higher modulus of elasticity and tensile strength.

2. Experimental

2.1. Materials

Polyethrsulphone (PES) (Ultrason E 6020P) was provided by BASF Corporation. Used 2-acrylamido-2-methylpropane sulfonic acid (commercially available as the AMPS®, a registered trade name of Lubrizol Corp.), N,N′-Methylenebis (acrylamide) (MBAA), N-Methyl-2-pyrrolidone (NMP) (99 % purity), copper (II) chloride dihydrate (99% purity), cadmium chloride (99% purity), nickel chloride hexahydrate (97% purity), hydrochloric acid, and sodium hydroxide were obtained from Sigma-Aldrich. The 2-hydroxy-1-[4-(2-hydrox-yethoxy)phenyl]-2-methyl-1-propanone (Irgacure 2959) was used as the photoinitiator (PI) and was kindly provided by Ciba SC. All chemicals were used as received without further purification. Distilled water was used for all of the experiments in the coagulation bath to prepare asymmetric membranes. Milli-Q deionized water was used to prepare stock solutions for heavy metal adsorption.

2.2. The preparation of the membranes

The hydrogel filled PES membranes were prepared by the modification of the liquid phase inversion [17]. The process was modified by incorporating AMPS and a crosslinking agent, MBA, in the polymer casting solution and copolymerizing them before the immersion precipitation and final solidification step. A 30 wt% of PES in NMP was prepared by mixing at 80°C for 12 h. The solutions of AMPS, MBAA, and PI in NMP were prepared by mixing components in cooled amber vials and protected from ambient light prior to the reaction. Each solution for making membranes was prepared by mixing a given quantity of PES with a solution of photopolymerizable components just prior to the casting. All of the prepared solutions were transparent, confirming the complete miscibility of the components. The amount of each component per 1 g of PES in the reaction mixture for the preparation of all the membranes is given in Table 1. PES concentration in the solutions prepared for casting was expressed as weight percentage of polymer per 100 g of total solution.

AMPS concentration was calculated in mmol per g of the final dry membrane at a theoretical 100% reactant conversion. The concentration of the crosslinking agent was presented in mol % based on the AMPS concentration. Membrane compositions are presented in Table 2. The prepared solutions were cast on a glass plate using a 7.62 cm-wide film applicator with a 200 µm gap (BYK-Gardner). In order to protect the reaction mixture from the ambient oxygen, the nitrogen was applied as a protection gas. The ultraviolet (UV) irradiation was applied through a transparent polyester film on thetop of the enclosure for 3 min. The exposure doze, mainly in the UVA region, was 1.5 J/cm^2, as measured by YK-35UV light meter. The UV exposure initiated polymerization and the crosslinking of AMPS to create a gel in the cast film. After the UV curing, the cast films were immersed in water bath to form membranes. Phase separation and solidification were completed in 10 min. After standing overnight, membrane samples were extracted from distilled water.

2.3. Characterization of samples

Effective yield of polymerized AMPS in membrane samples was determined by titration. A sample of wet membrane was immersed into 10 ml of 0.1 M HCl and mixed for 30 min.

Table 1
Components amounts per 1 g of PES in reaction mixture

Sample	AMPS, g	MBAA, g	Irgacure 2959, g
MSH1	0.61	0.05	0.007
MSH2	0.62	0.08	0.007
MSH3	1.09	0.13	0.013
MSH4	0.76	0.09	0.007

Table 2
The compositions of the membranes

Sample	PES, wt%	AMPS, mmol/g	MBAA, mol%
MSH1	13.2	1.76	12
MSH2	13.2	2.24	18
MSH3	15.0	2.40	15
MSH4	17.0	2.00	15

After thorough rinsing with deionized water until the conductivity was reduced to 1–2 µS/cm, 40 ml of 0.01 M NaOH was added and the suspension was stirred for 1 h to convert sulfonic groups from acidic into sodium form. Membrane pieces were dried in an oven at 100°C for 2 h to determine the mass of dry membrane, md. Aliquots (10 ml) of the spent NaOH solution were titrated with 0.01 M HCl in the presence of a couple of droplets of a phenolphthalein solution.

The morphology of membranes was investigated using a field emission scanning electron microscope (FESEM, TESCAN MIRA 3XMU) with fracture surfaces sputtered with gold for enhanced conductivity. Wet membrane samples were dried and fractured after cooling in liquid nitrogen. The size distribution of membrane pores was obtained through the analysis of the FESEM images by using the *Image Pro Plus 6.0* software. The tensile tests were performed on all of the prepared layered membranes in dry conditions of the samples, using an universal testing machine, Shimadzu Autograph AG-X (Japan), in accordance with the ASTM D3039 standard [18].

For the investigation of adsorption kinetics, membrane sample was immersed in 0.01 M HCl solution for 10 min, in order to convert sulfonic groups into the acidic form. Afterwards, the membranes were rinsed with deionized water until the conductivity dropped to 1–2 µS/cm. Samples were then placed in a Millipore stirred cell (Model 8050), filled with 1.5 mmol/l aqueous solution of Ni^{2+}, Cd^{2+}, or Cu^{2+} (50 ml), with contionuous stirring. Aliquots (0.5 ml) were taken on every 3 min from the solution and diluted to 10 ml with 0.5 M nitric acid. Four samples were tested for each metal, two samples were installed in the cell with the top and two with the bottom side facing the solution, respectively. The concentration of metal was determined by the flame absorption atomic spectroscopy (FAAS) using AAnalyst 300 PerkinElmer instrument.

3. Results and discussion

3.1. Titration and swelling ratio

Fig. 1 shows effective yield of polymerized AMPS and swelling ratio measured for asymmetric membranes. High copolymerization yield ensures presence of sufficient quantity of sulfonic groups that are able to bind cations of heavy metals; therefore, it was nessesary to determine which composition of a membrane represents the most promising candidate for further research. The results show that the effective conversion averaged from 51% for MSH1 up to 86% for MSH4 of the values expected based on the AMPS concentration in the initial solution. This would point out that a significant fraction of AMPS in MSH1 has either not been retained in the membrane, or was not available for titration. The PES concentrations in initial solutions were between 13.2 and 17 wt% and the yield of polymerized AMPS retained in the crosslinked gel was below 100% for all samples.

High swelling ratio enables effective mobility of the molecules inside the membrane, ensuring binding of heavy metal ions. As it can be seen from Fig. 1, highest swelling ratio showed MSH1, a membrane with the lowest concentration of AMPS. Higher concentrations of AMPS lead to an increase in copolymerization yield that reduces gel swelling.

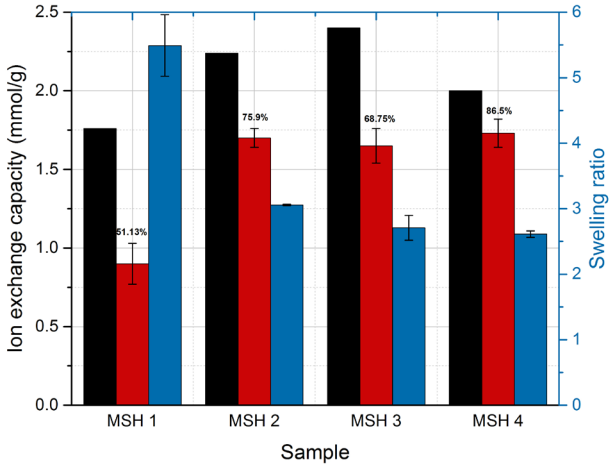

Fig. 1. Expected AMPS concentration in initial solution (■)effective yield of polymerized AMPS in asymmetric membranes(■) swelling ratio of MSH samples(■).

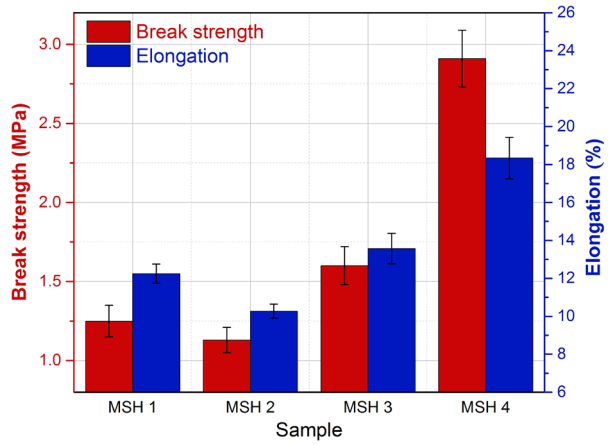

Fig. 2. Mechanical properties of MSH samples.

3.2. Tensile test

For practical use, it is necessary that swellable polymeric materials as adsorbents must withstand operating conditions. More precisely, the mechanical properties need to satisfy minimum application requirements. The results of tensile properties are presented in Fig. 2.

The tensile tests revealed that the Young's modulus of elasticity (E) was in the range of 0.25–0.76 MPa, The results of tensile strength are in the range from 1.29 MPa to 3.41 MPa and elongation at break from 10.27% to 18.34%, depending on the MSH composition (Table 3). The values of all of the tensile properties increased with the increase in the content of the polymer in the membrane. MSH4 stood out from the rest of the samples, with the value of the modulus of elasticity increased by 105% compared to the next highest E value, exhibited by MSH1.

As can be seen, the MSH4 exhibited the highest mechanical properties compared to the rest of the samples. According to the amounts of the starting components, it could be

Table 3
Tensile test results

Sample	*E*, MPa	ε, %	R_m, MPa
MSH1	0.37	13.93	1.41
MSH2	0.25	10.27	1.29
MSH3	0.26	13.57	1.81
MSH4	0.76	18.34	3.41

expected that the highest content of hydrogel would be in the MSH2. Consequently, the same sample was expected to have the lowest value of E, due to poor tensile properties of hydrogels (*E*~0.01–10 kPa) [19]. Gradual increase in the tensile properties before the leap for MSH4 indicated that a critical point was achieved with 17 wt% of PES, where it began to dominate in the failure mechanism. Taking into consideration composition of MSHs, their effective yield and the mechanical properties it is observed that the MSH4 is the most acceptable for use among the samples for adsorption tests.

3.3. FESEM analysis

FESEM images and pore size analysis of the MSH4 are presented in Figs. 3 and 4, respectively. The data obtained from *Image Pro Plus* software image analysis are based on the shape and size of the elements observed in the picture. The analysis was performed automatically, by the recognition of light and dark areas, corresponding to the pores and the surrounding polymer respectively [20]. The statistical analysis based on 7 FESEM micrographs showed that pore diameters were in the range from 0.04 μm to around 0.6 μm. This result indicated that active centers of the membrane would be available for metal cations in the swollen state, enabling good adsorption potential. FESEM confirmed that MSH has a typical asymmetric structure for membrane prepared by liquid phase inversion, containing dense skin on the top of a microporous support, as reported elsewhere [21]. The top side of the MSH supports the entire structure of this adsorbent preventing it's collapsing during the swelling (and adsorption).

3.4. Adsorption kinetics

One of the main properties of each adsorbent is its adsorption rate and the ability to bond targeted substances within the optimal time frame. The adsorption of the Cu^{2+}, Ni^{2+} and Cd^{2+} ions onto MSH4 was monitored, the change of concentration these elements was measured and their dependence on time is presented in Fig. 5. The curves for the bottom and top layers obviously differed,following the same pattern for all of the cations. High adsorption rate at the bottom side was in accordance with the expectations, because of its highly porous, hydrogel-rich nature; therefore, the adsorption rate was lower at skinned top side. The adsorption rate decreased over the time, before it reached the constant value.

In general, adsorption curve can be divided in three separate stages: linear, nonlinear, and saturation. For all tested

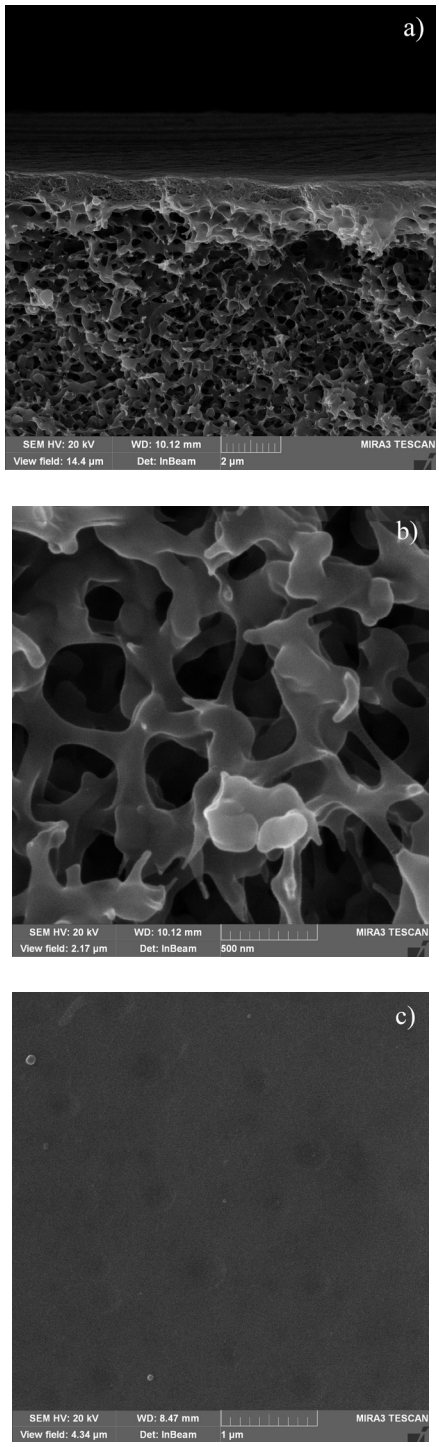

Fig. 3. FESEM images of a polyethersulfone MSH4 a) cross-section, b) bottom surface, c) top surface.

cations, the adsorption rate decreased with the increase in the degree of the adsorption. Therefore, maximal adsorption rates are achieved at the beginning i.e. for the low values of the adsorbed cations and high cations concentration in the solution. Due to the observed change in the adsorption rate with the progress of the adsorption process, it was reasonable to assume that the adsorption rate was con-

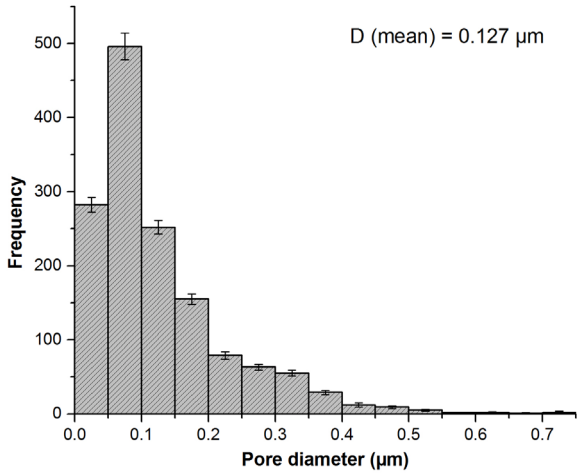

Fig. 4. Pore size distribution of the bottom side of MSH4.

trolled by the number of the available sites, rather than the diffusion rate [22]. To corroborate this assumption and find the kinetics model that would describe the best removal of the heavy metal cations onto the used MSH, the model – fitting method was used.

The basic principle of the model-fitting method is to classify chemical reaction in one of the five groups, according to the mechanism of the reaction. These groups are as follows: power law reaction, phase-boundary controlled reaction, first-order (F1), the Avrami equation described reaction and the diffusion-controlled reactions [23,24]. In the model-fitting method, the conversion rate curve presents the dependence of conversion rate α (the concentration of adsorbed heavy metal at time t per maximal adsorbed concentration at the end of the adsorption process) on time. Alternatively, time might be presented as the normalized value, where the reference value is the time when α reaches the value of 0.9 [22]. The obtained conversion curve is compared with the conversion curves predicted by the proposed models [25,26]. The best model to describe the heavy metal cations adsorption is the one with the lowest value of correlation coefficient (R^2). It is observed that in the case of the bottom side (hydrogel) the adsorption of all investigated heavy metal ions is controlled by the rate of the bidimensional movement of the boundary layer of the adsorbed phase, so called phase-boundary model (R2).

In that case, the following expression could be used:

$$\left[1-(1-\alpha)^{1/2}\right]=k_M t \quad (1)$$

where k_M stands for the model rate constant.

To confirm the fitting of this model, the dependence of $\left[1-(1-\alpha)^{1/2}\right]$ on t and $-\ln(1-\alpha)$ on t for adsorption of different heavy metals on the bottom and top side is presented in Fig. 6.

The dependences were linear, with the slope value of k_M for the adsorption of all three heavy metals on the top side of the membrane. On the other side, the same dependence was not straight line over the entire period of time

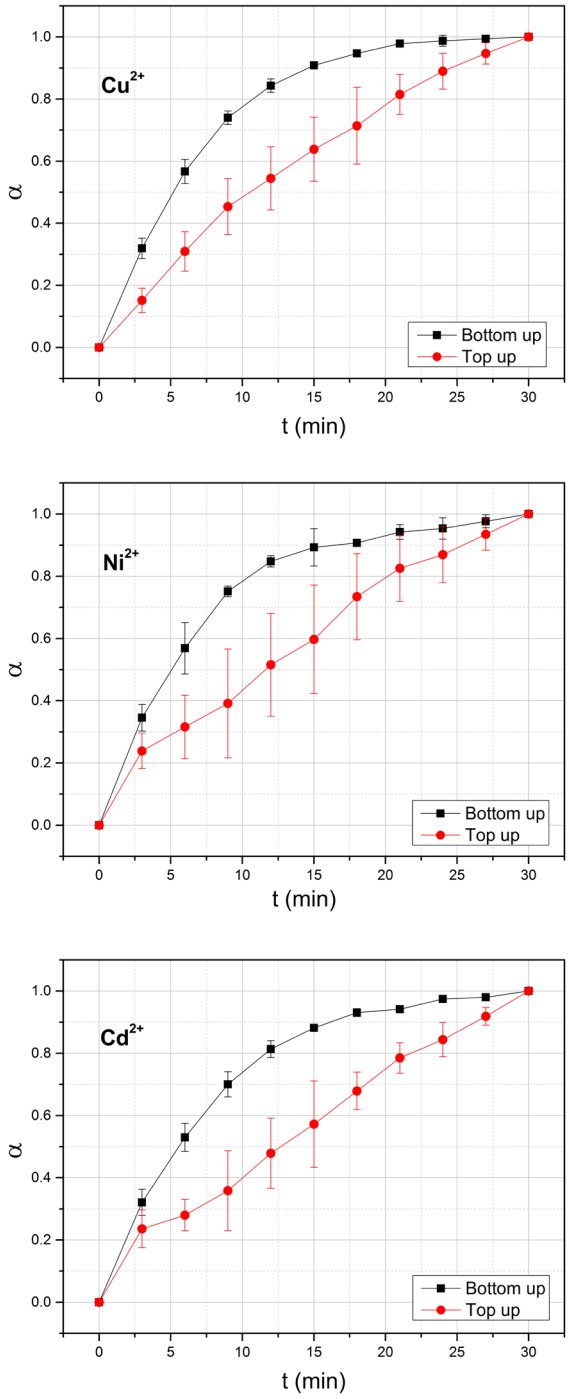

Fig. 5. Conversion curves for the adsorption of heavy metal cations: a) Cu^{2+} b) Ni^{2+} c) Cd^{2+}.

for the adsorption onto the bottom side of the membrane. The opposite was found for the first-order kinetics model (F1) model.

This implies that experimentally determined adsorption rate is in good accordance with the predicted model. Given that this conclusion is valid for the adsorption rates between 0 and 0.8, it is reasonable to conclude that the adsorption rate is described by Eq. (1).

Table 4
Relevant correlation coefficients (R^2) and kinetic parameter, k, for the adsorption kinetics

	R^2 model		F_1 model	
	k_2, min^{-1}	R^2	k_1, min^{-1}	R^2
Top				
Ni^{2+}	0.0269	0.997	0.0803	0.968
Cu^{2+}	0.0275	0.999	0.0869	0.962
Cd^{2+}	0.0251	0.996	0.0750	0.963
Bottom				
Ni^{2+}	0.0360	0.968	0.138	0.996
Cu^{2+}	0.0400	0.977	0.177	0.993
Cd^{2+}	0.0373	0.976	0.144	0.998

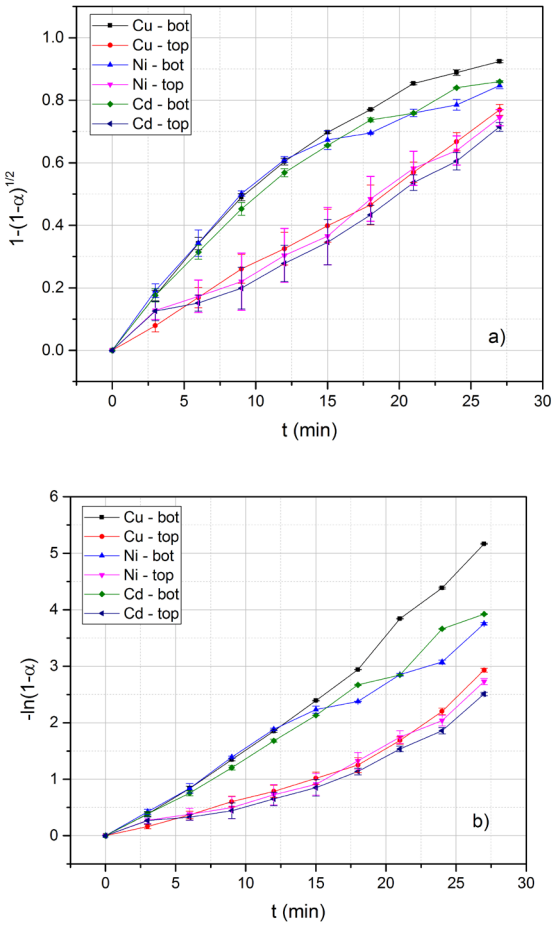

Fig. 6. Dependences a) $1–(1–\alpha)^{1/2}$ and b) $–\ln(1–\alpha)$ versus time for the heavy metal cations adsorption onto MSH4.

4. Conclusion

Asymmetric polyethersulphone-based membranes investigated in this study were prepared *via* novel method that includes combination of liquid phase inversion process with photopolymerization and monomer crosslinking. This method enabled 86% yield of polymerized monomer for the representative series MSH4, which is considered as a very high conversion. Tensile test has revealed that the membrane with the 17 wt% polyethersulphone showed a leap in tensile performance compared to the other samples. Failure mechanism of PES became dominant at that point, suggesting that this composition in the membrane offered optimal mechanical properties. These findings indicate that, by adjusting ratio of the PES towards hydrogel in the membrane, typical poor mechanical performance of hydrogels could be overcome, with retained adsorption ability. The statistical analysis of FESEM micrograph showed that achieved pore diameter range enabled good availability of the swollen membrane's active centers to the metal cations, promising good adsorption potential. Analysis of an adsorption capacity revealed that the bottom layer showed by far greater capacity compared to the top layer of the membrane, due to a presence of a hydrogel. Experimental results of the adsorption revealed that the bottom, hydrogel-rich layer submits to the first-order kinetics model, whereas the phase-boundary controlled reaction (contracting area) model was in accordance with the adsorption kinetics of the top, polymer rich side of the membrane.

Acknowledgement

This work has been supported by the Ministry of Education, Science and Technological Development of the Republic of Serbia under Projects: TR34011 and III 45019.

References

[1] S. Vakalis, K. Moustakas, D. Malamis, A. Sotiropoulos, S. Malamis, Assessing the removal of heavy metals in industrial wastewater by means of chemical exergy, Desal. Water Treat., 91 (2017) 146–151.
[2] S.E. Sherman, Q. Xiao, V. Percec, Mimicking complex biological membranes and their programmable glycan ligands with-dendrimersomes and glycodendrimersomes, Chem. Rev., 117 (2017) 6538–6631.
[3] E.A. Kamoun, E.-R.S. Kenawy, X. Chen, A review on polymeric hydrogel membranes for wound dressing applications: PVA-based hydrogel dressings, J. Adv. Res., 8 (2017) 217–233.
[4] B. Shimekit, H. Mukhtar, F. Ahmad, S. Maitra, Ceramic membranes for the separation of carbon dioxide - a review, T. Indian Ceram. Soc., 68 (2015) 115–138.
[5] N. Panapitiya, S. Wijenayake, D. Nguyen, C. Karunaweera, Y. Huang, K. Balkus Jr., I. Musselman, J. Ferraris, Compatibilized immiscible polymer blends for gas separations, Materials, 9 (2016) 643.
[6] M. Hofmanand R. Pietrzak, Copper ions removal from liquid phase by polyethersulfone (PES) membranes functionalized by introduction of carbonaceous materials, Chem. Eng. J., 215–216 (2013) 216–221.
[7] Q. Yang, N. Adrus, F. Tomicki, M. Ulbricht, Composites of functional polymeric hydrogels and porous membranes, J. Mater. Chem., 21 (2011) 2783–2811.
[8] N. Ghaemi, S.S. Madaeni, P. Daraei, H. Rajabi, S. Zinadini, A. Alizadeh, R. Heydari, M. Beygzadehand S. Ghouzivand, Polyethersulfone membrane enhanced with iron oxide nanoparticles for copper removal from water: Application of new functionalized Fe_3O_4 nanoparticles, Chem. Eng. J., 263 (2015) 101–112.
[9] P. Cay-Durgun, M.L. Lind, Nanoporous materials in polymeric membranes for desalination, Curr. Opin. Chem. Eng., 20 (2018) 19–27.

[10] J.H. Jhaveri, Z.V.P Murthy, Nanocomposite membranes, Desal. Water Treat., 57 (2015) 26803–26819.
[11] M. Jamadi, P. Shokrollahi, B. Houshmand, M.D. Joupari, F. Mashhadiabbas, A. Khademhosseini, N. Annabi, Poly (ethylene glycol)-based hydrogels as self-inflating tissue expanders with tunable mechanical and swelling properties, Macromol. Biosci., 17 (2017) 1600479.
[12] T. Marino, E. Blasi, S. Tornaghi, E. Di Nicolò, Alberto Figoli, Polyethersulfone membranes prepared with Rhodiasolv®Polarclean as water soluble green solvent, J. Membr. Sci., 549 (2018) 192–204.
[13] S. Montesanto, G.A. Mannella, F. Carfì Pavia, V. La Carrubba, V. Brucato, Coagulation bath composition and desiccation environment as tuning parameters to prepare skinless membranes via diffusion induced phase separation, J. Appl. Polym. Sci., 132 (2015) 42151.
[14] G.R. Guillen, Y. Pan, M. Li, E.M. V. Hoek, Preparation and characterization of membranes formed by nonsolvent induced phase separation: A review, Ind. Eng. Chem. Res., 50 (2011) 3798–3817.
[15] J. Ren, R. Wang, In: L.K. Wang, J.P. Chen, Y.-T. Hung, N.K. Shammas, Membrane and Desalination Technologies, Humana Press, New York, 2011, pp. 47–100.
[16] C. Zhao, J. Xue, F. Ranand S. Sun, Modification of polyethersulfone membranes - A review of methods, Prog. Mater. Sci., 58 (2013) 76–150.
[17] R.M. Boom, I.M. Wlenk, Th. van den Boomgaard, C.A. Smolders, Microstructures in phase inversion membranes. Part 2. The role of a polymeric additive, J. Membr. Sci., 73 (1992) 277–292.
[18] ASTM D3039/D3039M-17, Standard Test Method for Tensile Properties of Polymer Matrix Composite Materials, ASTM International, West Conshohocken, PA, 2017, www.astm.org.
[19] O. Okay, In: G. Gerlach, K.-F. Arndt, Hydrogel Sensors and Actuators, Springer-Verlag, Berlin Heidelberg 2010, pp. 1–14.
[20] N.Z. Tomić, Đ. Veljović, K. Trifković, B. Međo, M. Rakin, V. Radojević, R. Jančić-Heinemann, Numerical and experimental approach to testing the adhesive properties of modified polymer blend based on EVA/PMMA as coatings for optical fibers, Int. J. Adhes. Adhes., 73 (2017) 80–91.
[21] A. Stajčić, A. Nastasović, J. Stajić-Trošić, J. Marković, A. Onjia, F. Radovanović, Novel membrane-supported hydrogel for removal of heavy metals, J. Environ. Chem. Eng., 3 (2015) 453–461.
[22] C.H. Bamford, C.F.H. Tipper, Comprehensive Chemical Kinetics, Elsevier, Amsterdam, 1980.
[23] B. Adnadjevic, J. Jovanovic, Isothermal dehydration of the poly(acrylic -co-methacrylic acid) hydrogel, Ind. Eng. Chem. Res., 49 (2010) 11708–11713.
[24] A. Kodentsov, In: A. Paul, S. Divinski, Handbook of Solid State Diffusion, Vol. 2, Elsevier, Amsterdam 2017, pp. 277–337.
[25] S. Shin, S.I. Im, N.S. Nho, K.B. Lee, Kinetic analysis using thermogravimetric analysis for nonisothermal pyrolysis of vacuum residue, J. Therm. Anal. Calorim., 126 (2016) 933–941.
[26] W.-L. Wu, Q. Zhou, L. Yuan, X.-L. Deng, S.-R. Long, C.-L. Huang, H.-P. Cui, L.-S.Huo, J.-X. Zheng, Equilibrium, kinetic, and thermodynamic studies for crude structured-lipid deacidification using strong-base anion exchange resin, J. Chem. Eng. Data, 61 (2016) 1876–1885.